Disordered Polymorphic Modifications of Form I of Syndiotactic Polypropylene

Claudio De Rosa,* Finizia Auriemma, and Valeria Vinti

Dipartimento di Chimica, Università di Napoli "Federico II", Via Mezzocannone 4, 80134 Napoli, Italy

Received November 18, 1996; Revised Manuscript Received March 20, 1997[⊗]

ABSTRACT: The structural characterization of samples of syndiotactic polypropylene (s-PP) isothermally crystallized from the melt is presented. Form I of s-PP, with variable amount of disorder, is obtained at every crystallization temperature. The limit ordered modification, characterized by a fully antichiral packing along both axes of the unit cell and by a monoclinic symmetry $P2_1/a$, is obtained only at high values of the crystallization temperature (T_c > 135 °C). At crystallization temperatures in the range 120−135 °C, modifications characterized by disorder in the regular alternation of left- and right-handed helices along both axes of the unit cell are formed. At T_c < 120 °C, disorder in the stacking of *bc* layers of helices piled along *a*, implying a shift of *b*/4 among consecutive layers (*b*/4 shifts disorder), can also arise. The amount of both kinds of disorder depends on the crystallization temperature and increases in the as-prepared samples and in samples rapidly crystallized by quenching the melt. These samples are crystallized in a disordered modification which can be described by the statistical space group *Bmcm*. This model is characterized by a statistical disorder in the substitution of enantiomorphous helices in each site of the lattice, although local correlation about the chirality of neighboring chains may still be preserved. This correlation is lost in the long range because of the occurrence of the *b*/4 shifts disorder. A "continuum" of intermediate disordered modifications of form I exists among the limit statistical disordered form *Bmcm* and the limit ordered monoclinic form $P2_1/a$. In these modifications, the chains are already rotated around their axes by nearly 5° and displaced along *c* according to the packing pattern of the limit ordered modification $P2_1/a$.

Introduction

Syndiotactic polypropylene (s-PP) was first synthesized by Natta et al.[1] by using vanadium-based catalysts. As a consequence of the poor syndiospecificity of this catalytic system and of the scarcely interesting physicochemical properties of the polymer, s-PP has received in the past very little attention.

Highly stereoregular and regioregular s-PP has been synthesized only recently with new metallocene homogeneous catalysts;[2] the properties of this new s-PP have been greatly improved, and this has focused the research on s-PP, first of all, on clarifying the structure and the polymorphism of s-PP.

The polymorphic behavior of s-PP has been known for many years;[3−5] a stable modification, characterized by chains in **s**(2/1)2 helical conformation packed in an orthorhombic lattice,[3,4] and an unstable form, characterized by *trans* planar chains,[5] have been described in the past. Recent structural studies on s-PP based on electron diffraction,[6−9] X-ray diffraction,[10−17] and solid state ^{13}C NMR spectroscopy[18−21] have shown that the polymorphism of s-PP is more complex in the presence of new crystalline modifications as well as in the presence of different amounts of disorder in the crystalline phases, depending on the degree of stereoregularity and the mechanical and thermal history of the samples.

s-PP is characterized by two limiting ordered crystalline forms with chains in the **s**(2/1)2 helical conformation.

Form I (following the nomenclature proposed in ref 15) was found by Lovinger, Lotz, et al.;[6−9] it is the stable form of s-PP obtained under the most common conditions of crystallization (melt and solution crystallization) in powder samples and single crystals of s-PP. Form I is characterized by chains in **s**(2/1)2 helical conformation which are packed, in the ideal limit ordered structure, with an alternation of right-handed and left-handed helices along *a* and *b* axes of the unit cell. Lovinger, Lotz, et al.[6−9] proposed the space group *Ibca* for the crystal structure of form I; the axes of the helices are in the positions (0,0,*z*) and ($^1/_2$,0,*z*) of the orthorhombic unit cell having axes *a* = 14.5 Å, *b* = 11.2 Å, and *c* = 7.4 Å (Figure 1). The main X-ray peaks in the powder profile are at *d* = 7.25, 5.6, 4.70, and 4.31 Å (2θ = 12.2°, 15.8°, 18.8°, and 20.7°, Cu Kα).

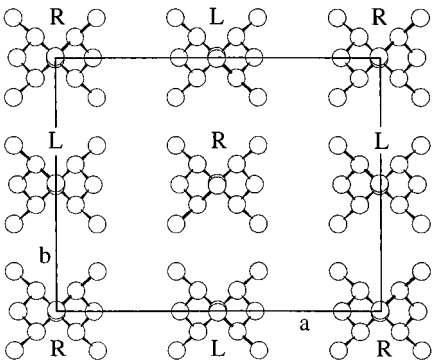

Figure 1. Orthorhombic model of packing of the limit ordered form I of s-PP corresponding to the space group *Ibca*.[6] The axes of the unit cell are *a* = 14.5 Å, *b* = 11.2 Å, and *c* = 7.4 Å. R, right-handed, L, left-handed helices.

The presence of the (011) reflection in the electron diffraction spectra of single crystals of s-PP grown at high temperature[9] and the splitting of the resonance of the methyl carbons observed in the solid state ^{13}C NMR spectra of annealed sample of s-PP,[19] showing X-ray diffraction patterns typical of form I, indicate that the crystal structure of form I is described only in a first approximation by the space group *Ibca*. For this space group, the (011) reflection is extinct, and all the methyl carbons are equivalent.

[⊗] Abstract published in *Advance ACS Abstracts,* June 1, 1997.

S0024-9297(96)01691-9 CCC: $14.00

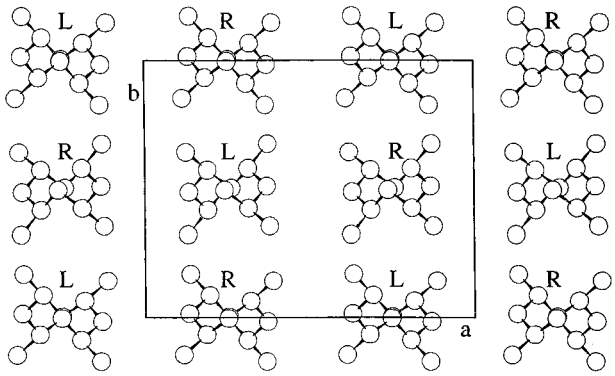

Figure 2. Monoclinic model of packing of the limit ordered form I of s-PP corresponding to the space group $P2_1/a$.[15] The axes of the unit cell are $a = 14.31$ Å, $b = 11.15$ Å, $c = 7.5$ Å and $\gamma = 90.3°$. R, right-handed, L, left-handed helices.

In a recent paper,[15] we analyzed the crystal structure of form I by refinement of the structure performed with the Rietveld method. We proposed[15] that helical chains are packed in the monoclinic unit cell with axes $a =$ 14.31 Å, $b = 11.15$ Å, and $c = 7.5$ Å, and $\gamma = 90.3°$, according to the space group $P2_1/a$ (Figure 2). Like in the space group *Ibca*, right- and left-handed helices alternate along the *a* and *b* axes of the unit cell, and the positions of the chain axes remain unaltered. The breaking of the symmetry in the space group results from a slight rotation of the chains around the chain axes of ±5°, shifts of consecutive *bc* layers of macromolecules of 0.13*c* along the chain axis, and a further shift, along *c*, of consecutive chains along *b* by 0.034*c*. This model of packing explains the presence of the (011) reflection in the electron diffraction spectra of single crystals of s-PP[9] and the splitting of the resonance of the methyl carbons observed in the solid state ^{13}C NMR spectra of form I of s-PP.[19]

Form II is obtained in annealed fiber samples of s-PP (often in mixtures with form I). It corresponds to the C-centered structure deduced by Corradini et al.[3,4] from the X-ray fiber diffraction spectra. This form is characterized by chains in **s**(2/1)2 helical conformation packed in the orthorhombic unit cell with axes $a = 14.5$ Å, $b = 5.60$ Å, and $c = 7.4$ Å. The axes of the helices are in the positions (0,0,*z*) and ($^1/_2$,$^1/_2$,*z*) of the unit cell, and the main X-ray peaks in the powder profile are at $d = 7.25$, 5.22, and 4.31 Å ($2\theta = 12.2°$, 17.0°, and 20.6°, Cu Kα).[4,10] The space group proposed for the limit ordered structure of form II is $C222_1$,[4] for which helices of the same chirality are included in the unit cell.

The polymorphism of s-PP is complicated by the fact that, depending on the degree of stereoregularity and the mechanical and thermal history of the samples, the various crystalline forms show different kinds and amounts of disorder in the crystalline packing.[6−12,17,20,21] For form I, broad peaks observed in the X-ray powder and fiber diffraction patterns[10] and streaks observed in the electron diffraction spectra[6−9] have been explained through disordered models characterized by a departure from the regular alternation of twofold helices of opposite chirality along the *a* and *b* axes of the unit cell,[10−12] as well as by a statistical mixture of crystals of form I and form II.[10−12] The latter kind of disorder has been observed in single crystals of s-PP obtained at low temperatures[8,9] and in fiber and powder specimens of s-PP.[10−12]

Limit ordered modification of form I, characterized by the monoclinic structure $P2_1/a$,[15] is obtained only when highly stereoregular samples of s-PP are crystallized from the melt at high temperatures (e.g. 140 °C)[15] or crystallized in single crystals grown at high temperatures (>130 °C).[8,9]

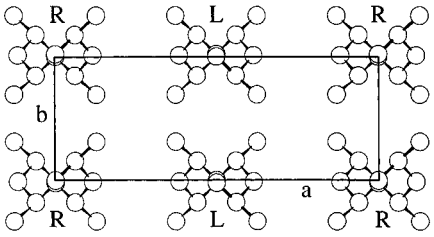

Figure 3. Orthorhombic model of packing of the form I of s-PP corresponding to the space group *Pcaa*.[6] The axes of the unit cell are $a = 14.5$ Å, $b = 5.6$ Å, and $c = 7.4$ Å. R, right-handed, L, left-handed helices.

Table 1. Molecular Weights, MW, Fully Syndiotactic Pentad Contents, [*rrrr*], and Melting Temperatures, T_m, of Four Samples of s-PP[a]

	MW	[*rrrr*] (%)	T_m (°C)
s-PP(1)	2.66×10^5	96.0	153
s-PP(2)	2.28×10^5	95.5	152
s-PP(3)	1.64×10^5	91.0	146
s-PP(4)	7.7×10^4	88.8	140

[a] These samples correspond to samples 1−4 of ref 25.

Single crystals of s-PP grown at low temperature (<130 °C), powder samples rapidly precipitated from solution, and samples crystallized by quenching the melt present a departure from the ideal, fully antichiral packing of Figures 1 and 2, as revealed by the weakness or, in same cases, by the absence of the (211) reflection at $d = 4.70$ Å ($2\theta = 18.8°$, Cu Kα) in the electron and X-ray diffraction patterns.[6,9,10] For these samples, Lovinger, Lotz, et al.[6] have proposed a structure with antichiral packing of chains only along the *a* axis; the structure should be represented by a unit cell with axes $a = 14.5$ Å, $b = 5.60$ Å, and $c = 7.4$ Å, and by the space group *Pcaa* if the fully symmetry of the chains is left, or $Pca2_1$ if the symmetry of the chains is not preserved[6] (Figure 3). The calculated structure factors for the model of Figure 3 (space group *Pcaa*), reported in ref 10, indicate that the structure needs to be refined. Indeed, the calculated intensities of the (201) and (221) reflections (the Miller indices are given for the unit cell with $b = 11.2$ Å) at calculated spacings $d = 5.179$ ($2\theta =$ 17.1°) and 3.802 Å ($2\theta = 23.4°$), respectively, are high; these reflections are absent in the X-ray powder diffraction profiles of these samples.[10]

In this paper, a structural characterization of samples of s-PP crystallized in modifications of form I, presenting variable amounts of disorder, is presented. The kind and the amount of the disorder, which depend on the crystallization temperature, are analyzed by comparison between the experimental and calculated X-ray diffraction profiles.

Experimental Section

Materials and Methods. The s-PP samples were supplied by Montell.

The polymer samples were synthesized with syndiospecific homogeneous catalyst composed of isopropylidene(cyclopentadienyl)(9-fluorenyl)zirconium dichloride and methylaluminoxane.[2] The samples are highly syndiotactic, with fully syndiotactic pentad contents [*rrrr*] in the range 96−89%. The molecular weights, MW, the syndiotactic pentad contents, [*rrrr*], and the melting temperatures of four samples of s-PP are reported in Table 1.

Samples of s-PP in form I were obtained by isothermal crystallization from the melt. The as-prepared samples were

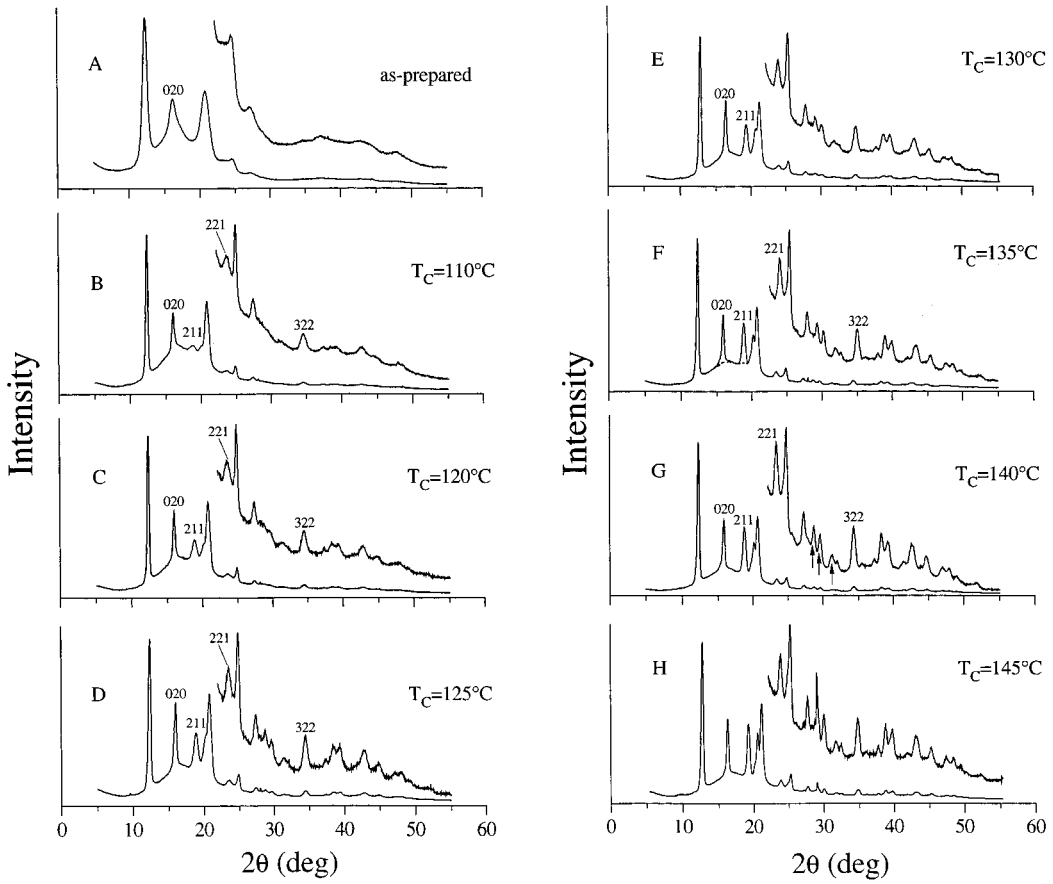

Figure 4. X-ray powder diffraction patterns of s-PP(1) samples isothermally crystallized from the melt at the indicated crystallization temperatures T_c. The region of $2\theta > 22°$ is shown on an enlarged intensity scale. The dashed lines shown in part F delimit the area of the (211) and (020) Bragg diffraction peaks from which the order parameter R is calculated. The indices hkl of the reflections are given for the unit cell of form I of figure 1 or 2.

melted at ~200 °C and kept for 5 min at this temperature in a N_2 atmosphere; they were then rapidly cooled to the crystallization temperature, T_c, and kept at this temperature, still in a N_2 atmosphere, for a time (t_c) long enough to allow complete crystallization at T_c. The samples were then cooled to room temperature and analyzed by wide-angle X-ray diffraction.

The melting temperatures of Table 1 were obtained with a differential scanning calorimeter (Perkin Elmer DSC-7) with scans in a flowing N_2 atmosphere and heating rates of 10 °C/min.

X-ray powder diffraction patterns were obtained at room temperature with an automatic Philips diffractometer using Ni-filtered Cu Kα radiation. The profiles were recorded with a continuum scan of the Bragg angle 2θ or, for high values of 2θ, with a step scan procedure. The count time for each step was equal to 60 s/step, and the step was 0.04° (2θ).

An estimation of the crystallinity index, X_c, of the samples was obtained from the X-ray powder diffraction profiles by measuring the intensity of the diffraction of the crystalline (I_c) and amorphous (I_a) phases: $X_c = I_c/(I_c + I_a)$.

An evaluation of the degree of order present in the structure of form I was done by measuring the ratio between the intensities of the (211) and (020) reflections, at $2\theta = 18.8°$ and 15.8°, respectively: $R = I(211)/I(020)$. The intensities of the (211) and (020) reflections were measured from the area of the corresponding diffraction peaks above the diffuse halo in the X-ray powder diffraction profiles (see Figure 4).

Calculations. For the limit ordered structures as well as for the disordered structure which can be described in terms of a statistical space group, the calculated X-ray diffraction profiles were obtained by multiplying the diffraction intensity, I_{hkl}, for each $2\theta_{hkl}$ value by a Cauchy function:

$$I_{\mathrm{calc},2\theta_i} = \sum_{hkl} I_{hkl}\Omega(2\theta_i - 2\theta_{hkl})$$

where the sum is extended over all hkl reflections with Bragg angles $2\theta_{hkl}$ close to the profile point $2\theta_i$ and $\Omega(2\theta_i - 2\theta_{hkl})$ is the Cauchy function. The latter has a half-height width regulated by the function:

$$H = [U\tan^2(\theta) + V\tan(\theta) + W]^{1/2}$$

where the values of U, V, and W were optimized in order to reproduce the half-height width of the peaks in the experimental profiles. The amorphous contribution, evaluated by the X-ray diffraction pattern of amorphous polypropylene, was scaled and summed to the calculated intensity $I_{\mathrm{calc},2\theta i}$.

For the calculations of the X-ray diffraction profiles of the structural model in which the order is kept only in the short range and lost in the long range, according to a suitable pattern, only structural models including disorder developing along one lattice direction were considered. The formulas used for these calculations are reported and developed elsewhere.[17,22] For our goals, it is enough that crystallites of size distributed according to a Bernoullian law were considered in the calculations, and their average dimensions were nearly 100 Å along a and b and nearly 50 Å along c.

Results and Discussion

The X-ray powder diffraction patterns of the as-prepared sample s-PP(1) and of samples of s-PP(1) obtained by isothermal crystallizations from the melt at various temperatures T_c are reported in Figure 4. It is apparent that, at each temperature, crystallization in form I always occurs. This is demonstrated by the presence, in the X-ray diffraction patterns of Figure 4, of (020) and (211) reflections at $2\theta = 15.8°$ and 18.8°, respectively, and by the absence of the (110) reflection at $2\theta = 17°$ typical of form II, as revealed for the first

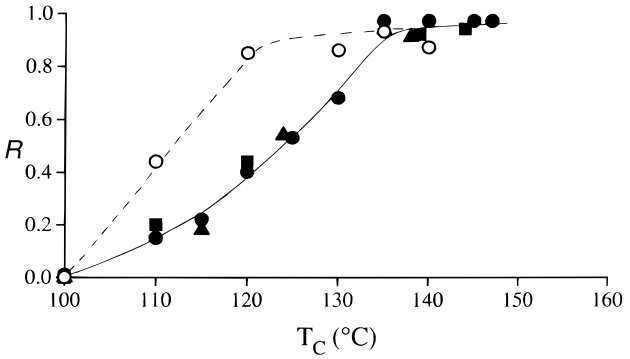

Figure 5. Values of the order parameter R of the s-PP samples of Table 1 crystallized from the melt, reported as a function of the crystallization temperature T_c. (●) s-PP(1); (■) s-PP(2); (▲) s-PP(3); (○) s-PP(4).

time by Lovinger, Lotz, et al.[6] The Miller indices of the (211) and (020) reflections of form I are given for the unit cell of Figure 1 or 2. The Miller indices of the (110) reflection of the form II are given for the unit cell of form II with $b = 5.6$ Å.

We recall that the (211) reflection at $2\theta = 18.8°$ is typical of the packing characterized by the regular alternation of twofold helices of opposite chirality along the a and b axes (Figures 1 and 2).[6] This reflection is absent in the X-ray powder diffraction pattern of the as-prepared sample (Figure 4A), whereas it is present in the X-ray diffraction patterns of the melt-crystallized samples, and its intensity rises with the crystallization temperature T_c (Figure 4B−H).

The profiles of Figure 4 indicate that, with increasing crystallization temperature, more ordered crystals of form I are obtained. At high temperature, $T_c = 135-140$ °C, the limiting ordered form I, corresponding to the monoclinic structure of Figure 2, is formed.

The intensity of the (211) reflection at $2\theta = 18.8°$ can be used as a measure of the degree of order present in the crystals of form I. Precisely, since the (020) reflection is constant with T_c, we use the ratio between the intensity of the (211) and (020) reflections, at $2\theta = 18.8°$ and 15.8°, respectively, $R = I(211)/I(020)$, in order to eliminate any dependence on the crystallinity and the thickness of the samples.

The values of R of the samples of Figure 4 are reported in Figure 5 as a function of T_c. R increases with T_c from $R = 0$ to a constant value $R \approx 1$.

Similar results are obtained for the other samples of s-PP in Table 1 with lower stereoregularity (s-PP(2), s-PP(3), and s-PP(4)). For instance, the X-ray powder diffraction patterns of the as-prepared sample s-PP(4) and of samples of s-PP(4) obtained by isothermal crystallizations from the melt at various temperatures T_c are reported in Figure 6. Although the as-prepared sample s-PP(4) is essentially in form II, as indicated by the presence of the (110) reflection at $2\theta = 17°$ in the pattern of Figure 6A,[20,21] the melt-crystallized samples are in form I.

The values of R for all the samples in Table 1, crystallized from the melt, are also reported in Figure 5 as a function of T_c. For each sample, R increases with T_c from $R = 0$ to $R \approx 1$.

For s-PP samples of high stereoregularity (s-PP(1), s-PP(2), and s-PP(3)), the limiting ordered monoclinic structure of form I (Figure 2, space group $P2_1/a$, with regular alternation of left- and right-handed helices along a and b), characterized by an X-ray diffraction pattern with nearly equal intensity of the (211) and

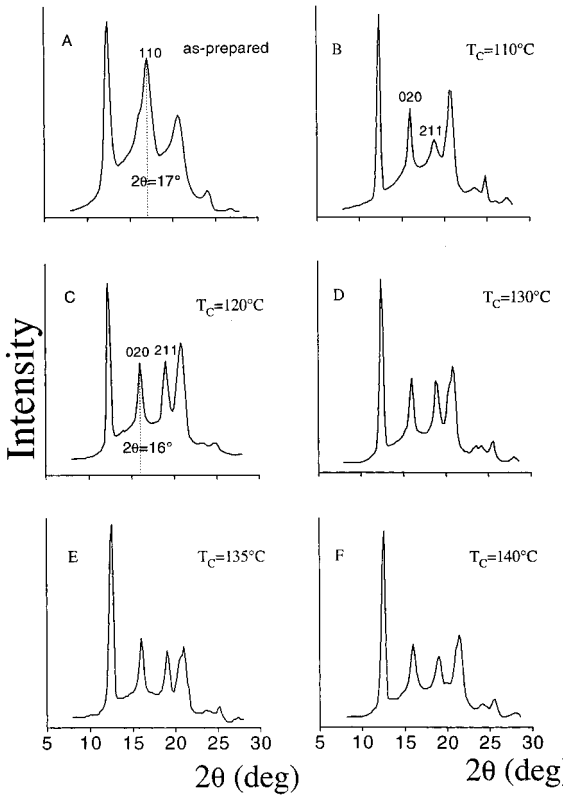

Figure 6. X-ray powder diffraction patterns of s-PP(4) samples isothermally crystallized from the melt at the indicated crystallization temperatures T_c. The indices of the (110) reflection are given, in A, for the unit cell of form II with $b = 5.6$ Å, whereas the indices of the (020) and (211) reflections are given, in B−F, for the unit cell of form I with $b = 11.2$ Å.

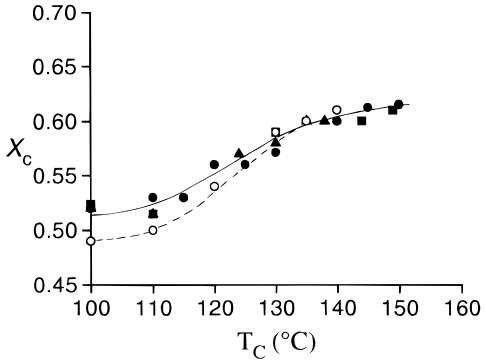

Figure 7. Values of the crystallinity X_c of the s-PP samples of Table 1 crystallized from the melt, reported as a function of the crystallization temperature T_c. (●) s-PP(1); (■) s-PP(2); (▲) s-PP(3); (○) s-PP(4).

(020) reflections ($R \approx 1$, Figure 4H), is obtained starting from a crystallization temperature of nearly 135 °C. Owing to the lower melting temperature of the sample s-PP(4), having lower stereoregularity, the limiting ordered structure of form I is already obtained at $T_c \approx 120$ °C (Figure 5). For all samples at higher values of T_c, only a slight increase of the crystallinity occurs, as shown in Figure 7, where the crystallinity index of the melt-crystallized samples is reported as a function of T_c.

It is worth noting that studies on isothermally melt-crystallized samples of s-PP have been already reported in literature.[23,24] In both papers,[23,24] poor disordered modifications of form I were obtained, and X-ray diffraction profiles with high intensity of the (211) reflection at $2\theta = 18.8°$ were never obtained, as a conse-

quence. Indeed, Loos et al.[23] observed that, in their sample of s-PP, no crystallization was obtained, even after several days, at temperatures above 120 °C. Crystallization was observed only when performing the melt crystallization with the self-seeding procedure, but a poor disordered modification of form I was obtained, as revealed by the low intensity of the (211) reflection in the X-ray diffraction patterns of these samples.[23] Moreover, Rodriguez-Arnold et al.[24] obtained melt-crystallized samples characterized by X-ray diffraction patterns with the presence of the (211) reflection only for samples of s-PP of low molecular weight. They concluded that the formation of the fully antichiral packing along both axes of the unit cell is not only dependent on crystallization temperature but is also associated with molecular weight and may, indeed, be controlled through crystallization kinetics.[24]

From our data of Figures 4−6, it is apparent that we have obtained more ordered modifications of form I, with $R \approx 1$, very near to the limit ordered monoclinic form $P2_1/a$. In our samples, crystallization in the ordered form I occurs at high T_c without the self-seeding procedure and also for samples of high molecular weight.

All the samples crystallized at low temperatures are characterized by the presence of disorder ($0 \leq R < 1$).

Disorder in the As-Prepared Samples. The X-ray powder diffraction pattern of the as-prepared s-PP(1) sample (Figure 4A), as well as that of the sample crystallized by quenching the melt (not shown), is characterized by the absence of the (211) reflection at $2\theta = 18.8°$ ($R = 0$). These samples are therefore characterized by disorder, implying the departure from the regular alternation of helices of opposite chirality along the *a* and *b* axes. This disorder does not affect the packing of the chains. Indeed, the samples have still high values of crystallinity (~50%), and the corresponding X-ray diffraction profiles present a sharp (020) reflection with high intensity (Figure 4A). We recall that the (020) reflection is characteristic of the packing of the chains with axes in the positions (0,0,*z*) and ($^1/_2$,0,*z*) of the unit cell[6] (Figures 1−3).

For these samples, Lovinger, Lotz, et al.[6] proposed the ordered structural model of Figure 3, corresponding to the space group *Pcaa* (or $Pca2_1$). We have already shown in ref 10 that some kind of disorder should be present in the structure. Indeed, structure factors calculations for the space group *Pcaa*, reported in ref 10, show that the calculated intensities of the (201) and (221) reflections (the Miller indices are given for the unit cell with $b = 11.2$ Å) at calculated spacings $d = 5.179$ ($2\theta = 17.1°$) and 3.802 Å ($2\theta = 23.4°$), respectively, are high; these reflections are absent in the X-ray diffraction profile of Figure 4A. These discrepancies are more evident in the comparison between the experimental X-ray powder diffraction pattern of the as-prepared s-PP(1) sample of Figure 4A and the calculated profile for the model of Figure 3, space group *Pcaa*, shown in Figure 8. It is apparent that, besides the (201) and (221) reflections, also the calculated broad peaks at $2\theta = 29.4°$ (Miller indices, for the unit cell with $b = 11.2$ Å, of the contributing reflections (022), (420), (122)), at $2\theta = 31.6°$ ((222) and (421) reflections), at $2\theta = 34.5°$ ((322) reflection), and at $2\theta = 38.4°$ ((422) and (341) reflections) (curves b,b′ in Figure 8) are absent or have weak intensities in the experimental profile (curves a,a′ in Figure 8).

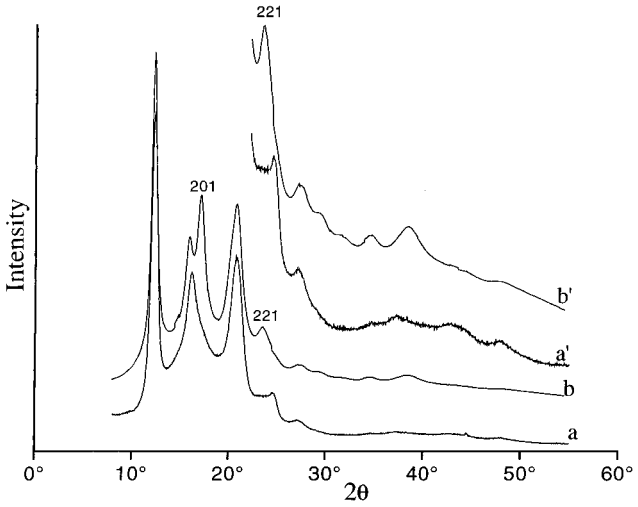

Figure 8. Comparison between the experimental X-ray powder diffraction profile of the as-prepared s-PP(1) sample (curve a) and the calculated profile for the model of packing of figure 3 for the space group *Pcaa* (curve b). The experimental (curve a′) and calculated (curve b′) profiles for $2\theta > 22°$ on an enlarged intensity scale are also reported. The indices of the (201) and (221) reflections are given for the unit cell with $b = 11.2$ Å.

The absence of the (201) and (221) reflections in the experimental X-ray powder diffraction pattern of the as-prepared sample (Figures 4A and 8a) indicates that some kind of disorder is present in the structure. A possible disorder could be related to the statistical substitution of right- and left-handed helices in each site of the unit cell, giving rise to a departure from the fully antichiral packing along both axes. The limit statistical disordered structure can be described by the unit cell with axes $a = 14.5$ Å, $b = 5.6$ Å, $c = 7.4$ Å and by the statistical space group *Bmcm*.[10] The (201) and (221) reflections (the Miller indices are given again for the unit cell with $b = 11.2$ Å) are extinct for the space group *Bmcm*, and a good agreement between the calculated structure factors, already reported in ref 10, and experimental intensities is obtained. A comparison between the calculated X-ray diffraction profile, for the space group *Bmcm*, and the experimental pattern of the as-prepared s-PP(1) sample is reported in Figure 9. It is apparent that also the peaks calculated for the space group *Pcaa* at $2\theta = 29.4°$, 31.6°, 34.5°, and 38.4° (Figure 8) are absent or very weak in the profile calculated for the space group *Bmcm* (Figure 9, curves b,b′) in accordance with the experimental profile (Figure 9, curves a,a′).

It is worth noting, however, that models in which a local correlation about the chirality of neighboring chains is preserved might well be suitable for describing the structure of the as-prepared sample. Indeed, antichiral packing of first neighboring chains may still be preserved locally and lost in the long range also because of the occurrence of disorder in the stacking of *bc* layers of helices piled along *a*, implying a shift of *b*/4 among consecutive *bc* layers.[8,9] This kind of disorder occurs in the single crystals of s-PP grown at low temperatures, as suggested by Lovinger, Lotz, et al.[8,9]

Disorder in the Melt-Crystallized Samples. In all the samples crystallized from the melt at temperatures lower than 135 °C (or lower than 120 °C for the sample s-PP(4)), modifications with a degree of disorder depending on T_c ($0 < R < 1$) are obtained. These modifications are intermediate among the limit disor-

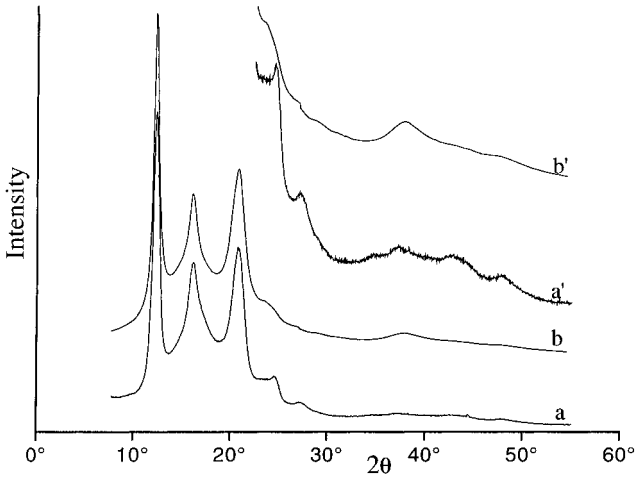

Figure 9. Comparison between the experimental X-ray powder diffraction profile of the as-prepared s-PP(1) sample (curve a) and the calculated profile for the disordered model of packing corresponding to the statistical space group *Bmcm* (curve b). The experimental (curve a′) and calculated (curve b′) profiles for $2\theta > 22°$ on an enlarged intensity scale are also reported.

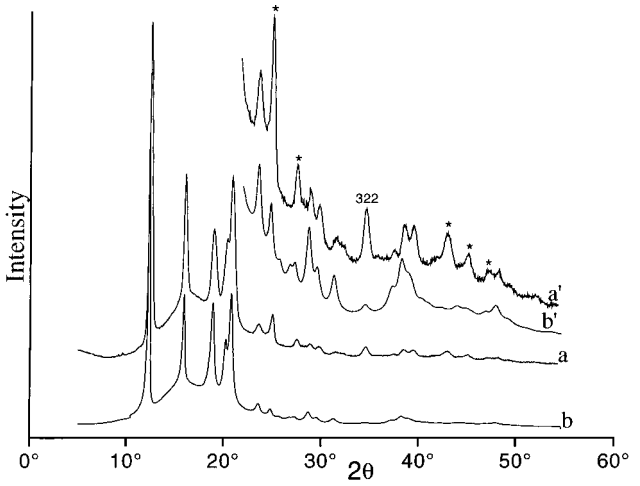

Figure 10. Comparison between the experimental X-ray powder diffraction profile of the sample s-PP(1) crystallized from the melt at 130 °C (curve a) and the calculated profile for the model of packing of Figure 1 corresponding to the space group *Ibca* (curve b). The experimental (curve a′) and calculated (curve b′) profiles for $2\theta > 22°$ on an enlarged intensity scale are also reported.

dered modification *Bmcm* and the limit ordered one $P2_1/a$.

The increase of the order parameter R with T_c indicates that a gradual improvement of the order in the regular alternation of left- and right-handed helices along the axes of the unit cell occurs.

We recall that, in the limit ordered monoclinic modification of form I, space group $P2_1/a$ (Figure 2), besides the fully antichiral packing, a local order corresponding to a rotation of the chains of nearly 5° around the chain axes and slight displacements of the chains along *c* is present, giving rise to a breaking of the orthorhombic symmetry.[15] In the high-symmetry orthorhombic model, corresponding to the space group *Ibca* (Figure 1), the chains have not the freedom to rotate or translate along *c*, so that they only alternate their chirality along the axes of the unit cell.

In this section, we shall analyze two kinds of disorder possibly present in the intermediate modifications: (a) disorder arising from random rotations of the chains and slight translations of the chains along the chain axes and (b) disorder arising from defects in the regular alternations of left- and right-handed helices along the axes of the unit cell.

We first analyze the disorder related to the presence of random rotations of the chains and slight random translations of the chains along the chain axis, around the average values corresponding to the position of the chains in the structural model *Ibca*. Disordered modifications characterized by this kind of disorder and presenting already the order in the alternation of helices of opposite chirality could be described by an average structural model corresponding to the space group *Ibca*.

An analysis of the X-ray diffraction profiles in the region of high values of the Bragg angle 2θ (Figure 4) can be used to test this hypothesis. It is apparent from Figure 4 that, in the pass from the as-prepared sample (Figure 4A) to the melt-crystallized samples, the (322) reflection at $2\theta = 34.2°$ appears immediately (Figure 4B). Moreover, the (221) reflections at $2\theta = 23.5°$ and the peaks at $2\theta = 28.7°$ ((411) and (022) reflections), at $2\theta = 29.6°$ ((231) and (420) reflections), and at $2\theta = 31.2°$ ((312) and (222) reflections), not observed or very weak in the pattern of the as-prepared sample (Figure 4A), increase their intensities with the increase of the crystallization temperature (Figure 4B−H; the latter three diffraction peaks are indicated with arrows in Figure 4G).

A comparison between the calculated X-ray diffraction profile for the structural model corresponding to the space group *Ibca* and one of the experimental profiles of Figure 4 (for instance, that corresponding to $T_c = 130$ °C) is reported in Figure 10.

In all the X-ray diffraction patterns of Figure 4, always the (322) reflection is present at $2\theta = 34.2°$; this reflection is extinct in the space group *Ibca*, and in the calculated profile of Figure 10 (curves b,b′), only a very weak diffraction peak is present at $2\theta \approx 34°$. Moreover, in the X-ray diffraction profiles of Figure 4, diffraction peaks are always present, indicated with asterisks in Figure 10, at $2\theta = 24.8°$ ((400) and (002) reflections), at $2\theta = 27.2°$ ((321) and (202) reflections), at $2\theta = 42.6°$ ((242), (522) and (432) reflections), at $2\theta = 44.6°$ ((342) reflection), and at $2\theta = 47.1°$ ((423) reflection), which have instead very weak intensities or are absent in the calculated profile of Figure 10 (curves b,b′) for the space group *Ibca*.

This analysis indicates that the disordered intermediate modifications, obtained at $T_c < 135$ °C, cannot be properly described by the structural model corresponding to the space group *Ibca*.

The presence of the (322) reflection at $2\theta = 34.2°$ in all the X-ray diffraction profiles of Figure 4B−H (also at low crystallization temperatures), and the absence of this reflection in the calculated profile for the structural model corresponding to the space group *Ibca* (Figure 10 b,b′), indicate that the packing pattern characterized by the relative rotations of the chains around their axes and translations of the chains along *c*, typical of the limit ordered $P2_1/a$ modification, develops in the melt-crystallized samples already at low crystallization temperatures.

The disorder present in these modifications is, therefore, mainly due to defects in the regular alternation of left- and right-handed helices along the axes of the unit cell.

It is worth noting that Lovinger, Lotz, et al.[8,9] performed a detailed study on the disorder occurring

in single crystals of s-PP obtained at different temperatures. This disorder consists of the occurrence of *b*/4 shifts between consecutive *bc* layers of helices piled along *a*, producing in the electron diffraction photographs streaks along the *h* reciprocal coordinate of (020) and (211) reflections.[8,9] This kind of disorder should produce an increase of the background scattering underlying those reflections and a decrease of their maximum heights in the X-ray powder diffraction profiles, whereas the intensity of the (200) reflections should remain constant. In Figure 4, we observe that, for $T_c \geq 120$ °C, the intensity ratio among the maximum heights of (200) and (020) reflections remains almost constant, whereas the intensity of the (211) reflection increases with T_c. In samples obtained at $T_c < 120$ °C, instead, some diffuse scattering underlying the (020) reflection is probably present. This indicates that, for the latter samples, stacking faults implying *b*/4 shifts among consecutive *bc* layers piled along *a* occur, whereas for samples crystallized at $T_c \geq 120$ °C, other kinds of disorder may occur.

For the samples crystallized at $T_c \geq 120$ °C, defects can arise from the substitution of enantiomorphous helices in some site of the lattice (the statistical substitution of enatiomorphous helices in all sites of the lattice gives rise to the limit disordered model *Bmcm*, probably representative of the structure of the as-prepared sample). Models in which the alternation in chirality among first neighboring chains is effective in the short range, and lost in the long range, are approximate with models where the disorder develops along one lattice direction only, *a* or *b* in the example reported here.

Examples of models of packing which present disorder in the regular alternation of left- and right-handed helices along *a* or *b* are reported in Figure 11A,B, respectively. In these models, the chains are rotated by ∼5° around their axes, with respect to the model *Ibca*, and consecutive *bc* layers of macromolecules along *a* are shifted by 0.14*c* along the chain axis, as occurs in the limit ordered $P2_1/a$ modification (Figure 2). For the sake of simplicity, the further shift of consecutive chains along *b* of 0.034*c* along the chain axis, present in the limit ordered $P2_1/a$ modification,[15] were not considered. Indeed, in the models of Figure 11, the chains are arranged according to the packing pattern of the orthorhombic space group *Pbca*, which well describes the most important features of the crystal structure of form I (see ref 15).

In the model of Figure 11A, the disorder in the alternation of left- and right-handed helices develops along *a*; ordered *bc* layers of macromolecules, composed of chains of opposite chirality that alternate along *b*, are piled along *a* with probability p_a that two first neighboring helices, facing along *a*, are of opposite chirality, like in the limit ordered model $P2_1/a$, and with probability $1 - p_a$ that these helices are isochiral. In the model Figure 11B, the disorder develops along the *b* axis; ordered *ac* layers of macromolecules, composed of chains of opposite chirality that alternate along *a*, are piled along *b* with probability p_b that two first neighboring helices, facing along *b*, are of opposite chirality and with probability $1 - p_b$ that these helices are isochiral.

The calculated X-ray powder diffraction profiles for the models of Figure 11A,B are reported in Figures 12 and 13, respectively, for different values of the probabilities p_a and p_b.

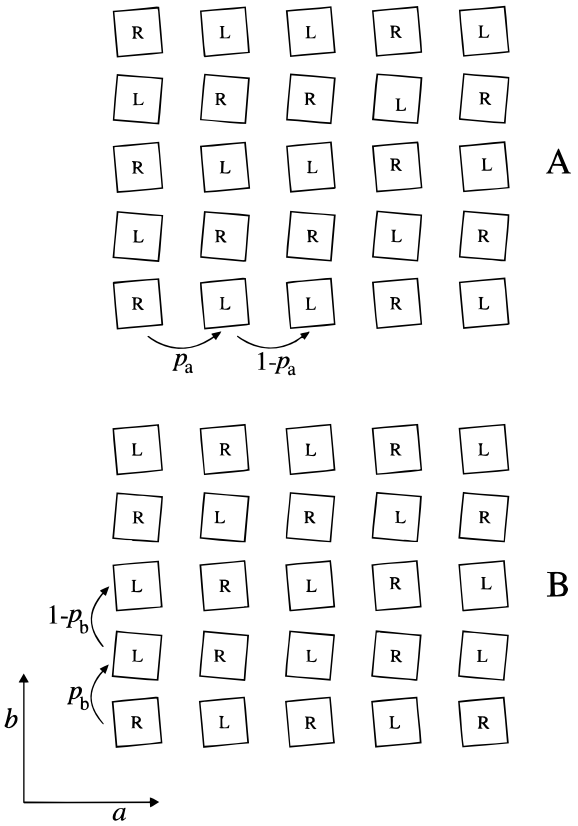

Figure 11. Models of packing of chains of s-PP for the disordered modifications of form I. The chains are represented by rectangles whose vertices are the carbon atoms of the methyl groups. The chains are rotated by ∼5° around their axes with respect to the position in the structural model *Ibca*, and consecutive *bc* layers of chains along *a* are shifted by 0.14*c* along *c*, like in the limit ordered modification $P2_1/a$ (Figure 2). R, right-handed, L, left-handed helices. p_a and p_b are the probabilities that two first neighboring helices, facing along *a* (A), or facing along *b* (B), respectively, are of opposite chirality.

It is apparent that, with increasing degree of disorder (and decreasing p_a and p_b), the diffraction peak (211), typical of the ordered structure ($p_a = 1$, Figure 12D, and $p_b = 1$, Figure 13D), becomes lower and broader. It disappears already for $p_a = 0.8$ (Figure 12A) and $p_b = 0.8$ (Figure 13A). Moreover, for the model of Figure 11B, with increasing disorder, the intensity of the (221) reflection at $2\theta = 23.4°$ also decreases, as occurs in the experimental profiles of Figures 4, and it becomes very low already for $p_b = 0.8$ (Figure 13A). As discussed above, this reflection is absent in the as-prepared samples. The intensity of the equatorial (020) reflection at $2\theta = 15.8°$ remains instead high with the increase of the disorder (Figures 12 and 13), as occurs in the experimental patterns (Figure 4). Some experimental X-ray diffraction profiles of Figure 4 are reported in Figure 14, after the subtraction of the amorphous halo, for a better comparison with the calculated profiles of Figures 12 and 13. A good agreement for each T_c is apparent. The values of the order parameter *R*, evaluated from the calculated X-ray powder diffraction profiles of Figures 12 and 13, are reported in Figure 15 as a function of the probability *p* (p_a and p_b). It is apparent that the theoretical trend of *R* vs *p* is very similar to the experimental trend, up to $T_c = 135$ °C, of *R* vs T_c (compare Figures 15 and 5).

The calculations of Figures 12 and 13 show that the models of Figure 11 can account for the experimental X-ray diffraction patterns of the samples of s-PP crystallized at temperatures below 135 °C and above 120

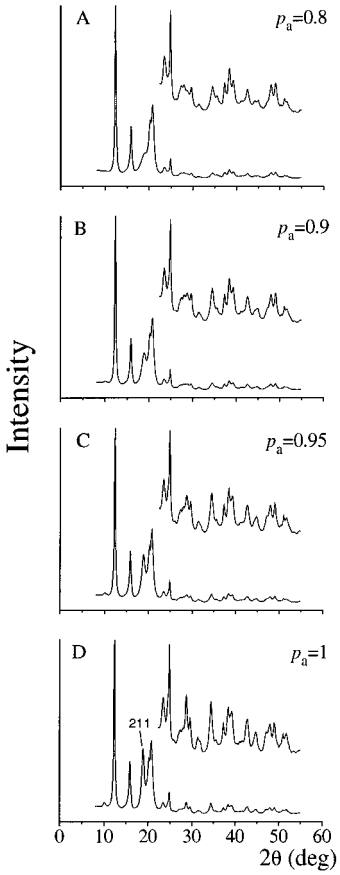

Figure 12. Calculated X-ray powder diffraction profiles for the model of Figure 11A for the indicated values of the probability p_a.

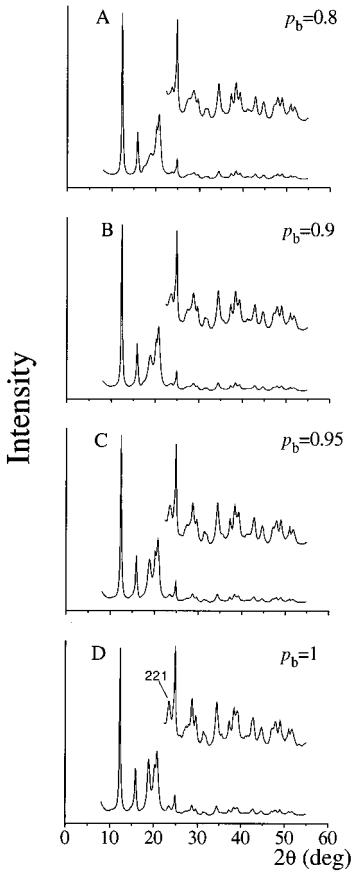

Figure 13. Calculated X-ray powder diffraction profiles for the model of Figure 11B for the indicated values of the probability p_b.

°C ($0 < R < 1$), where the intensity of the (211) reflection at $2\theta = 18.8°$ is always lower than that of the limit ordered modification, and the equatorial (020) reflection at $2\theta = 15.8°$ remains strong and sharp. They indicate that the disorder in the regular alternation of left- and right-handed helices develops along both *a* and *b* axes of the unit cell.

It is worth noting that disordered models similar to that of Figure 11A with the chains rotated by ∼5° around their axes, without any displacements of *bc* layers along *c*, give calculated X-ray diffraction profiles similar to those of Figure 12 but with a very low intensity of the (322) reflection. This indicates that the displacements of 0.14*c* along the chain axis of consecutive *bc* layers of chains, typical of the limit ordered modification $P2_1/a$, is the most important feature which characterizes also the disordered intermediate modifications.

For samples crystallized at $T_c < 120$ °C, disorder can also arise from defects in the stacking of *bc* layers of chains along *a*, which produce a local arrangement of the chains as in the C-centered form II of s-PP.[11,12] Figure 16 shows the calculated X-ray powder diffraction profiles for disordered models of packing, where *bc* layers of helices follow each other along *a* like in the limit ordered *Ibca* model structure with probability p_c, or shifted by *b*/4 with probability $(1 - p_c)$. It is apparent that, upon increasing the disorder, the intensities of the (020) and (211) reflections decrease in agreement with the experimental data of Figure 4 for $T_c < 120$ °C. In the calculated patterns of Figure 16, the intensity of the (221) reflection remains constant. This probably indicates that disorder of Figure 11B also occurs for these samples.

We recall that disorder implying *b*/4 shifts among consecutive *bc* layers piled along *a*[11,12] can account for experimental electron diffraction data on single crystals of s-PP grown at low temperatures,[9] which show diffuse scattering along the *h*11 layer line when diffuse scattering is present also along the *h*20 layer line (like, for instance, in the case of single crystals grown at 100 °C[9]); these spectra show strong and discrete reflections corresponding to indices (211) when strong and discrete reflections corresponding to indices (020) are present (like, for instance, in the case of single crystals grown at 140 °C[9]).

Conclusions

Form I of s-PP crystallizes from the melt in different modifications characterized by variable amounts of disorder depending on the crystallization temperatures. The ratio *R* between the intensities of (211) and (020) reflections at $2\theta = 18.8°$ and 15.8°, respectively, has been used as a measure of the degree of order present in the sample crystallized in form I.

The limit ordered modification characterized by a monoclinic symmetry $P2_1/a$ and a value of *R* nearly equal to 1, is obtained only at a high value of the crystallization temperature ($T_c > 135$ °C). At lower crystallization temperatures, modifications characterized by disorder in the regular alternation of left- and right-handed helices along the axes of the unit cell are formed ($0 < R < 1$). In these disordered modifications, the chains are already rotated around their axes of ∼5° and displaced along *c*, according to the packing pattern of the limit ordered modification $P2_1/a$, even at lower crystallization temperatures. Comparisons between

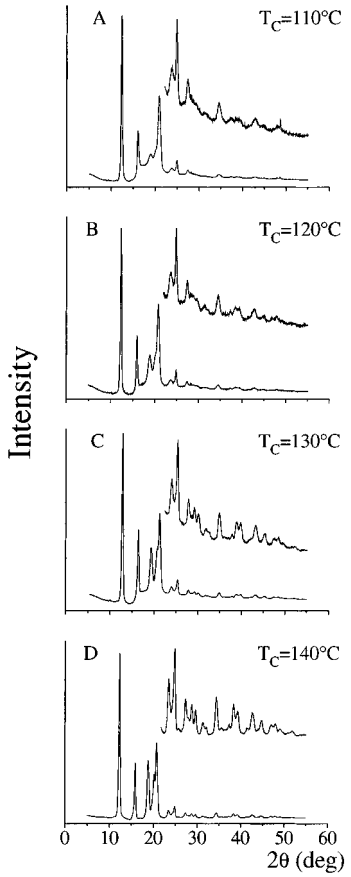

Figure 14. X-ray powder diffraction patterns of the s-PP(1) samples crystallized from the melt at the indicated crystallization temperatures T_c after the subtraction of the amorphous halo.

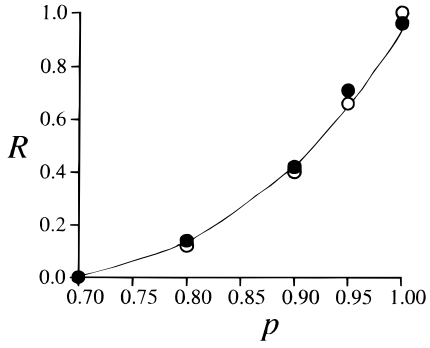

Figure 15. Values of the order parameter R, evaluated from the calculated X-ray diffraction profiles of Figure 12, for the model of Figure 11A (●), and from the calculated X-ray diffraction profiles of Figure 13, for the model of Figure 11B (○), reported as a function of the probability p ($= p_a = p_b$).

calculated and experimental X-ray diffraction profiles show that, in these modifications, the disorder in the regular alternation of left- and right-handed helices develops along both the *a* and *b* axes of the unit cell. This model of disorder accounts for the X-ray diffraction profiles of samples isothermally crystallized at temperature below 135 °C and above 120 °C, where the intensity of the (211) reflection at $2\theta = 18.8°$ is lower than that of the limit ordered modification, and the equatorial (020) reflection at $2\theta = 15.8°$ remains strong and sharp at each value of the crystallization temperature. We recall that the substitution of left- and right-handed helices in the sites of the lattice does not affect the positioning of the methyl groups;[12] therefore, the disorder concerns mainly the positioning of the backbone atoms. At $T_c < 120$ °C, disorder can also arise from defects in the stacking of *bc* layers of chains along *a*, implying *b*/4 shifts among consecutive layers, as in the single crystals of s-PP grown at low temperatures.[8,9]

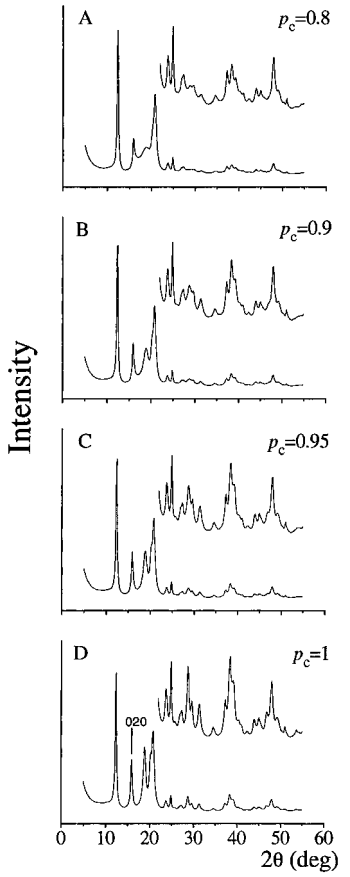

Figure 16. Calculated X-ray powder diffraction profiles for a disordered model of packing in which *bc* layers of helices follow each other along *a* like in the limit ordered *Ibca* model structure with probability p_c, or shifted by *b*/4 with probability $(1 - p_c)$, for the indicated values of the probability p_c.

The amount of the disorder in the regular alternation of left- and right-handed helices along the axes of the unit cell and in the stacking of *bc* layers of chains depends on the crystallization temperature and increases in the as-prepared samples and in samples rapidly crystallized by quenching the melt. These samples are crystallized in a disordered modification which can be described by the statistical space group *Bmcm*. This model is characterized by a statistical disorder in the substitution of enantiomorphous helices in each site of the lattice, although local correlation about the chirality of neighboring chains may still be preserved. This correlation is lost in the long range because of the occurrence of the *b*/4 shifts disorder.

A "continuum" of intermediate disordered modifications of form I exists among the limit statistical disordered form *Bmcm* and the limit ordered monoclinic form $P2_1/a$.

Acknowledgment. We thank Dr. M. Galimberti of Montell Ferrara for supplying the polymer samples. Financial support from the "Ministero dell'Università e della Ricerca Scientifica e Tecnologica", is gratefully acknowledged.

References and Notes

(1) Natta, G; Pasquon, P.; Zambelli, A. *J. Am. Chem. Soc.* **1962**, *84*, 1488.

(2) Ewen, J. A.; Jones, R. J.; Razavi, A.; Ferrara, J. D. *J. Am. Chem. Soc.* **1988**, *110*, 6255.
(3) Natta, G.; Corradini, P.; Ganis, P. *Makromol. Chem.* **1960**, *39*, 238.
(4) Corradini, P.; Natta, G.; Ganis, P.; Temussi, P. A. *J. Polym. Sci., Part C* **1967**, *16*, 2477.
(5) Natta, G.; Peraldo, M.; Allegra, G. *Makromol. Chem.* **1964**, *75*, 215.
(6) Lotz, B.; Lovinger, A. J.; Cais, R. E. *Macromolecules* **1988**, *21*, 2375.
(7) Lovinger, A. J.; Lotz, B.; Davis, P. D. *Polymer* **1990**, *31*, 2253.
(8) Lovinger, A. J.; Davis, D. D.; Lotz, B. *Macromolecules* **1991**, *24*, 552.
(9) Lovinger, A. J.; Lotz, B.; Davis, D. D.; Padden, F. J. *Macromolecules* **1993**, *26*, 3494.
(10) De Rosa, C.; Corradini, P. *Macromolecules* **1993**, *26*, 5711.
(11) Auriemma, F.; De Rosa, C.; Corradini, P. *Macromolecules* **1993**, *26*, 5719.
(12) Auriemma, F.; De Rosa, C.; Corradini, P. *Rend. Fis. Accad. Lincei* **1993**, *4*, 287.
(13) Chatani, Y.; Maruyama, H.; Noguchi, K.; Asanuma, T.; Shiomura, T. *J. Polym. Sci., Part C* **1990**, *28*, 393.
(14) Chatani, Y.; Maruyama, H.; Asanuma, T.; Shiomura, T. *J. Polym. Sci., Polym. Phys.* **1991**, *29*, 1649.
(15) De Rosa, C.; Auriemma, F.; Corradini, P. *Macromolecules* **1996**, *29*, 7452.
(16) Auriemma, F.; De Rosa, C.; Ruiz de Ballesteros, O.; Vinti, V.; Corradini, P. *J. Polym. Sci.*, in press.
(17) Auriemma, F.; De Rosa, C.; Ruiz de Ballesteros, O.; Corradini, P. *Macromolecules*, in press.
(18) Sozzani, P.; Galimberti, M.; Balbontin, G. *Makromol. Chem. Rapid Commun.* **1993**, *13*, 305.
(19) Sozzani, P.; Simonutti, R.; Galimberti, M. *Macromolecules* **1993**, *26*, 5782.
(20) Auriemma, F.; Born, R.; Spiess, H. W.; De Rosa, C.; Corradini, P. *Macromolecules* **1995**, *28*, 6902.
(21) Auriemma, F.; Lewis, R. H.; Spiess, H. W.; De Rosa, C. *Macromol. Chem.* **1995**, *196*, 4011.
(22) Allegra, G. *Nuovo Cimento* **1962**, *23*, 502. Allegra, G.; Bassi, I. W. *Gazz. Chim. Ital.* **1980**, *110*, 437.
(23) Loos, J.; Buhk, M.; Petermann, J.; Zoumis, K.; Kaminsky, W. *Polymer* **1996**, *37*, 387.
(24) Rodriguez-Arnold, J.; Zhang, A.; Cheng, S. Z. D.; Lovinger, A. J.; Hsieh, E. T.; Chu, P.; Johnson, T. W.; Honnell, K. G.; Geerts, R. G.; Palackal, S. J.; Hawley, G. R.; Welch, M. B. *Polymer* **1994**, *35*, 1884.
(25) Balbontin, G.; Dainelli, D.; Galimberti, M.; Paganetto, G. *Makromol. Chem.* **1992**, *193*, 693.

MA961691F